

Fetal MRI: A pictorial essay

Sapna Rathee, Priscilla Joshi, Abhimanyu Kelkar, Nagesh Seth

Department of Radiodiagnosis, Bharati Hospital, Pune, Maharashtra, India

Correspondence: Dr. Sapna Rathee, C/O SR Century Public School, Delhi Rohtak Road, Bahadurgarh - 124 507, Jhajjar, Haryana, India.
E-mail: dr.sapnarathee@gmail.com

Abstract

Ultrasonography (USG) is the primary method for antenatal fetal evaluation. However, fetal magnetic resonance imaging (MRI) has now become a valuable adjunct to USG in confirming/excluding suspected abnormalities and in the detection of additional abnormalities, thus changing the outcome of pregnancy and optimizing perinatal management. With the development of ultrafast sequences, fetal MRI has made remarkable progress in recent times. In this pictorial essay, we illustrate a spectrum of structural abnormalities affecting the central nervous system, thorax, genitourinary and gastrointestinal tract, as well as miscellaneous anomalies. Anomalies in twin gestations and placental abnormalities have also been included.

Key words: Anomalies; congenital; fetal magnetic resonance imaging; ultrasonography

Introduction

USG has routinely been used in the evaluation of obstetrical and gynecological conditions since the late 1950s. However, due to its limitations of a small field of view, operator dependence, a need for an additional imaging modality has emerged, especially in cases of oligohydramnios and obese patients. As MRI does not involve radiation, is safe for the fetus, and provides detailed structural anatomy, it has emerged as a suitable adjunct to USG.

MRI was first performed in 1983 for evaluation of the placenta and fetus.^[1] The main drawback of MRI was fetal motion which was overcome in the 1990s with the development of ultrafast sequences.^[2] According to the Safety Committee of the Society for MRI, no known biological risks have so far been proven to be associated with MRI. Acoustic noise and biological effects are the main safety concerns for fetal MRI. The noise intensity produced by gradients in fetal MRI can reach 120 dB. Fetal hearing damage, which is a potential hazard, has still not been confirmed in practice.^[3]

Fetal MRI is indicated in pregnant women when other non-ionizing diagnostic imaging methods are inadequate or when the examination provides important information that would otherwise require exposure to ionizing radiation.^[4] The quality of fetal MRI is comparable to postnatal MRI, facilitating discussion of surgical treatment options. Relative advantages and disadvantages of antenatal USG and MRI are described in Table 1.

Fetal MRI should be performed in the second or third trimester. As the teratogenic effects of MRI in early pregnancy are not confirmed and the multilayer structure of the cerebral parenchyma is appreciable after 16 weeks of gestation on a 1.5 T MR, MRI is best performed after completion of organogenesis (16 weeks).^[5] The patients are advised to fast for 4 h prior to the study, to reduce bowel peristalsis artifacts and to prevent postprandial fetal motion. Patients are asked to empty the urinary bladder prior to the study and positioned feet first supine or in left lateral decubitus position. A single-body matrix coil is often used over the abdomen and pelvis to improve the spatial resolution. No medication or sedation is required.

MR Protocol

MR studies are best performed on a MRI system with field strength of 1.5 T. Imaging is performed during free breathing with respiratory gating to avoid artifacts.

Initially, multiplanar T2-weighted (T2W) scout images are often obtained using 5-7-mm-thick slices with a 1- to 2-mm

Access this article online

Quick Response Code:



Website:
www.ijri.org

DOI:
10.4103/0971-3026.178326

gap and a large field of view, followed by a T2W_TSE sagittal sequence of the mother, to visualize the position of the fetus, placenta, and cervix as well as assess the uterus. Sequences should be performed in the coronal, sagittal, and axial planes through the region of interest for confirming/excluding the suspected fetal anomalies. This is followed by sequences through the rest of the fetus to rule out/detect associated anomalies. Ultrafast T2W sequences known as single-shot rapid acquisition with refocused echoes (i.e. single-shot fast spin-echo or half-Fourier acquired single-shot turbo spin-echo) are often used. Single images acquired in less than 1 s, decrease the artifacts from fetal motion. In addition to the regular T2W_TSE and balanced turbo field echo (BTFE) sequences for evaluating the fetus, T1-weighted image (T1WI) sequences of the fetal abdomen in the sagittal and coronal planes help to confirm the presence of meconium (which appears bright on T1WI) in the large bowel and rectum, up to the anal verge [Table 2]. It should be noted that BTFE, being a heavily T2W sequence, demonstrates fetal anatomy better at an early gestational age, as compared to the regular T2W sequence.

For detailed neurological evaluation, multiplanar T2W and BTFE sequences can be obtained. Ventricular atrial

Table 1: Advantages and disadvantages of fetal MRI and antenatal ultrasound

Antenatal ultrasound	Fetal MRI
Real-time display and noninvasive	No radiation, superior spatial and soft tissue resolution
Operator dependent	Relatively operator independent
Small FOV and difficulty in obtaining multiplanar views	Large field of view FOV and multiplanar capabilities
Poor image quality in oligohydramnios, maternal obesity	Better fetal anatomy delineation, independent of fetal position and maternal obesity
Reverberation artifacts, maternal bowel gas are problems	Poor visualization at <16 weeks gestation. Poor bone visualization, disadvantage in skeletal dysplasia and calcified lesions
Cost-effective	Expensive, time consuming, claustrophobia
Widely available	Limited availability

MR: Magnetic resource imaging, FOV: Field of view

Table 2: Sequences for fetal MRI

Sequence	Plane	FOV (mm)	Slice thickness (mm)	Gap (mm)	TR/TE (ms)	Matrix
BFFE_Survey	3-plane	450	15	10	7.7/4.6	224×256
T2W_TSE	3-plane	180	4	0.4	520/80	340×266
SSh_MRCP	3-plane	250	40	0	8000/900	296×238
BTFE_RT	3-plane	375	4	0.5	4.6/2.3	312×247
T1_TSE	Sagittal, coronal	375	5	1	10/4.6	252×151
BTFE_RLT	Sagittal	320	5	0	2.2/1.10	192×190

MRI: Magnetic resource imaging, BTFE: Balanced turbo field echo, T2W: T2-weighted, BFFE: Balanced fast field echo, TSE: Turbo spin echo, MRCP: Magnetic resonance cholangiopancreatography, RT: Respiratory triggering, RLT: Real time, TR/TE - Time to repeat/ Tome to echo

measurements are typically in the axial plane. Cavum septum pellucidum and corpus callosum (CC) must be identified. Age-appropriate sulcation and gyration is evaluated next. The tegmento-vermian angle [Figure 1] is measured on the midline sagittal image of the fetal brain. It is the angle formed by lines along the anterior surface of the vermis and the dorsal surface of the brainstem. The angle should be near zero. Large angles indicate elevation of the vermis due to the developmental anomalies of vermis. The cerebellar transverse diameter and cisterna magna are measured in axial images.

Indications

The most important indications of fetal MRI are evaluation of the fetus in suspected chromosomal syndromes/familial genetic disorders where USG is normal, confirmation of anomalies/findings detected on USG, and detecting/excluding associated anomalies. Fetal MRI can also assist in planning prenatal/postnatal intervention where necessary [Table 3].

Spectrum of anomalies

CNS anomalies

The most common indication for CNS imaging was ventriculomegaly, followed by suspected CC abnormalities, cerebellar anomalies, congenital infections, malformations of cortical development, and posterior fossa anomalies. Ventriculomegaly is defined as atrial width equal to or more than 10 mm on the sonogram. Figure 1 shows normal CC and brain anatomy.

CC anomalies

The CC is a midline cerebral structure consisting of white matter tracts connecting two cerebral hemispheres. Its formation starts at the 10th week of gestation with genu formation and is completed by 18-20th weeks with the formation of rostrum.^[6] It is seen as a C-shaped, curved hypointense structure on T2W images in the midsagittal plane [Figure 1]. Cerebral ventriculomegaly raises the suspicion of CC agenesis. MRI is superior to prenatal USG for evaluation of CC at any gestational age as it actually shows the CC, whereas ultrasonography (USG) relies on indirect signs like absence of cavum septum pellucidum for diagnosing CC anomalies. MR imaging features suggestive of CC agenesis are parallelization of lateral ventricles (Viking helmet sign), colpocephaly, and a high riding third ventricle [Figure 2].

Holoprosencephaly

It is characterized by lack of cleavage of prosencephalon.^[7] There is incomplete separation of two cerebral hemispheres. MRI is complementary to USG for confirmation and further evaluation of the subtypes of holoprosencephaly, i.e. lobar [Figure 3], semilobar, and lobar, in order of severity. The spectrum of findings in holoprosencephaly includes monoventricle, fusion of thalami, and absence of falx, CC, and optic tracts.

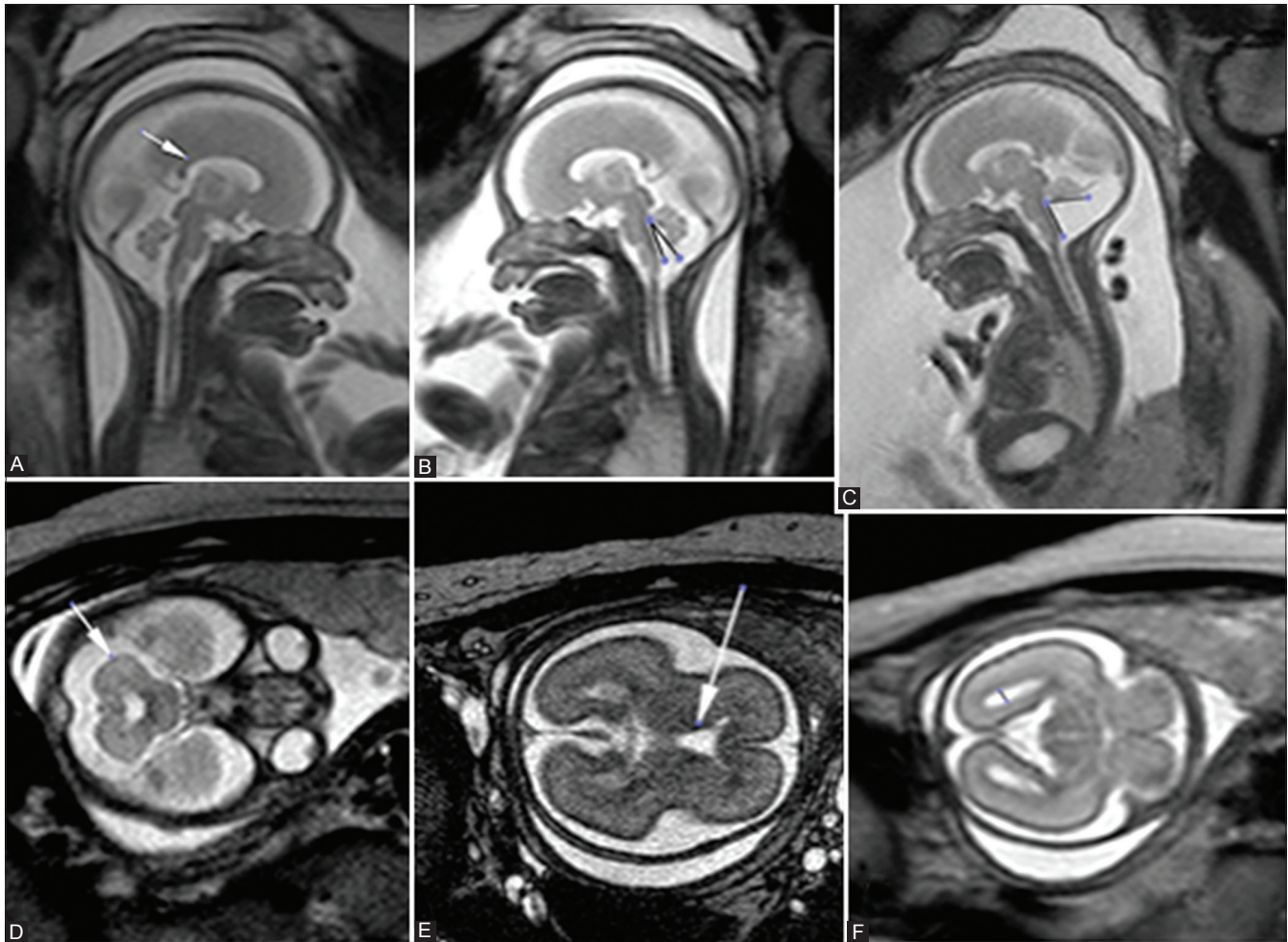


Figure 1 (A-F): Normal corpus callosum and brain anatomy. T2WI sagittal (A) image shows normal corpus callosum, (B) normal tegmento-vermian angle, and (C) shows increased angle in case of vermian hypoplasia. T2W axial (D) image shows normal cerebellum, cavum septum pellucidum (E and F) reveal normal ventricular size

Table 3: Fetal MRI indications

Fetal indications	Other indications
Confirmation/further evaluation of inconclusive/occult sonographic findings	Placental abnormalities like placenta previa, placenta accreta
Intrauterine growth retardation	Molar pregnancy
Oligohydramnios	Uterine leiomyoma
Evaluation in high-risk pregnancies with bad obstetric history	To assist in prenatal/postnatal intervention

MRI: Magnetic resource imaging

Associated anomalies include cleft lip, hypertelorism, encephaloceles [Figure 4], adrenal and cardiac anomalies.

Neural tube defects

These are a group of anomalies due to incomplete closure of the neural tube in early pregnancy. They include spina bifida, meningocele, meningomyelocele, and lipomeningomyelocele.

Anencephaly

It is a type of neural defect comprising absence of cranial vault and cortical tissue [Figure 5]. It can be associated with

spina bifida, congenital heart anomalies, skeletal anomalies, gastrointestinal anomalies, and diaphragmatic hernias.

Iniiencephaly

It is a neural tube defect, more common in females, with an incidence of 10 in 10,000.^[8] It is characterized by retroflexion of head, absence of occipital bones, spinal deformities, fusion of cervicothoracic vertebrae, and absence of neck causing upward turning of chin and face^[9] [Figure 6].

Chiari malformations

These are a group of disorders associated with congenital downward displacement of the cerebellum and brainstem, showing peg-like tonsillar herniation into the upper cervical canal on T2W images with a small posterior fossa. Four types are known. Chiari I is the commonest type with tonsillar herniation. Type II is associated with lumbosacral spinal myelomeningocele [Figure 7]. Type III is associated with a cervical/occipital encephalocele, and type IV is a variation of cerebellar hypoplasia.^[10] The limitation of USG

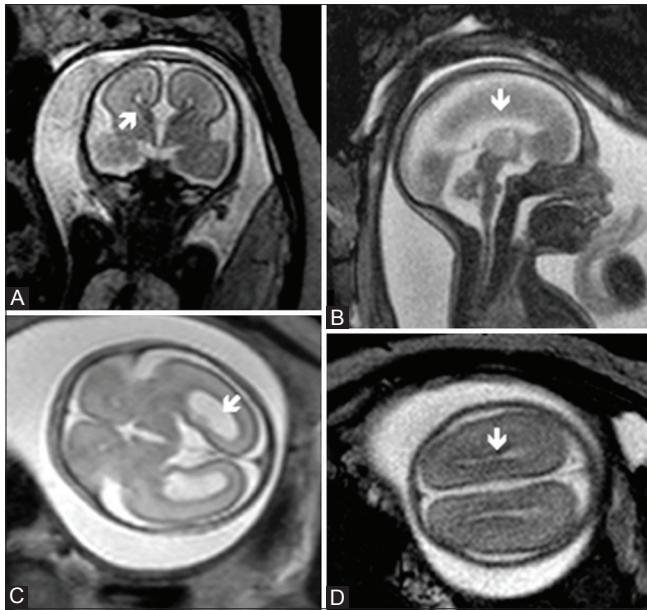


Figure 2 (A-D): Agenesis of corpus callosum at 22 weeks gestation. USG revealed colpocephaly. BTFE coronal image (A) shows a “high riding” third ventricle. T2W sagittal image (B) shows non-visualization of corpus callosum. T2W axial image (C) reveals colpocephaly and BTFE axial image (D) shows parallelization of lateral ventricles

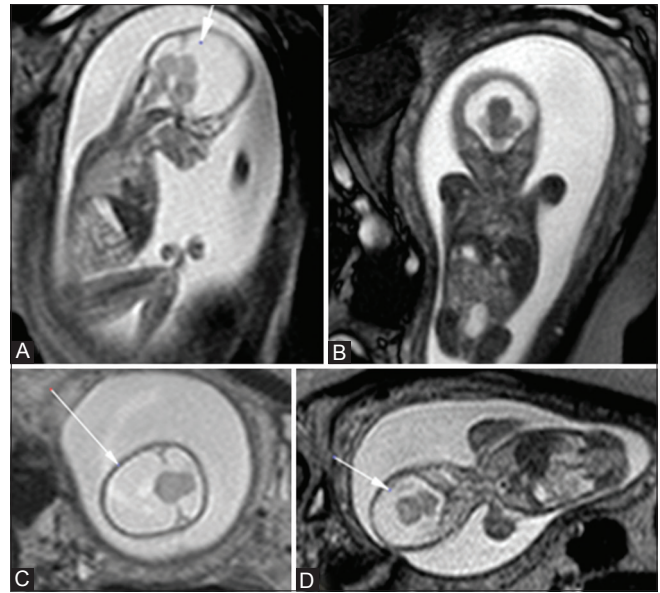


Figure 3 (A-D): Alobar holoprosencephaly in a fetus at 16 weeks. T2WI sagittal, (A) coronal, (B) axial, (carrows) and (D) images show central horseshoe-shaped monoventricle with fused thalami centrally. Absent falx/interhemispheric fissure as well as corpus callosum. A normal posterior fossa is seen

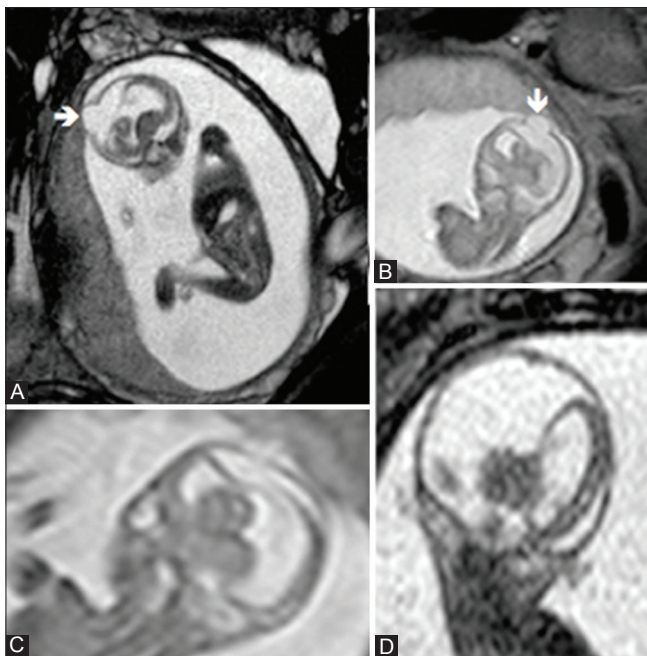


Figure 4 (A-D): Holoprosencephaly with encephalocele in a fetus at 16 weeks. T2WI sagittal (A-C) and coronal (D) images reveal dilated lateral ventricles. A cranial vault defect is seen toward the vertex (arrow)

in visualizing the posterior fossa and detecting tonsillar herniation has been overcome by fetal MRI.

Genitourinary tract anomalies

MRI scores over USG as fetal kidneys are well visualized and can be evaluated in the early gestational period as

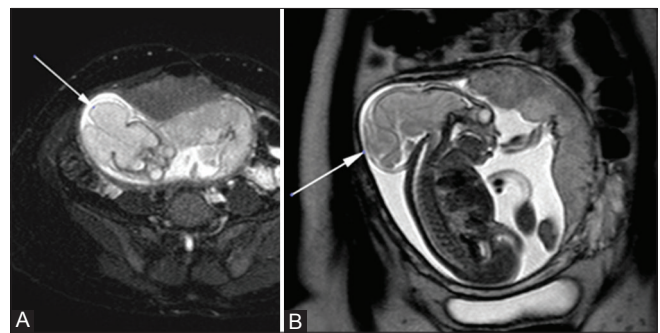


Figure 5 (A and B): Anencephaly in a fetus at 22 weeks. T2WI axial (A) and sagittal (B) images show absence of cranial vault and herniation of cerebral hemispheres

well as in the presence of scanty liquor. Oligohydramnios limits the assessment of genitourinary anomalies on USG due to the poor sonic window, thus making MRI a useful adjunct. Fetal ureters are not visualized on USG unless dilated. Hydronephrosis is the most common genitourinary abnormality detected on prenatal USG.^[11] Commonest causes of hydronephrosis are pelviureteric junction obstruction, vesicoureteral reflux, megaureter, and posterior urethral valves (PUVs).

Posterior urethral valves

It is the commonest cause of hydronephrosis and obstructive uropathy in male infants. On antenatal USG, the urethra shows a “keyhole” appearance with a distended urinary bladder and urethra proximal to valve [Figure 8]. Three types of PUVs were described in the past; however, at present, only one type is accepted (type I).^[12] Fetal MRI

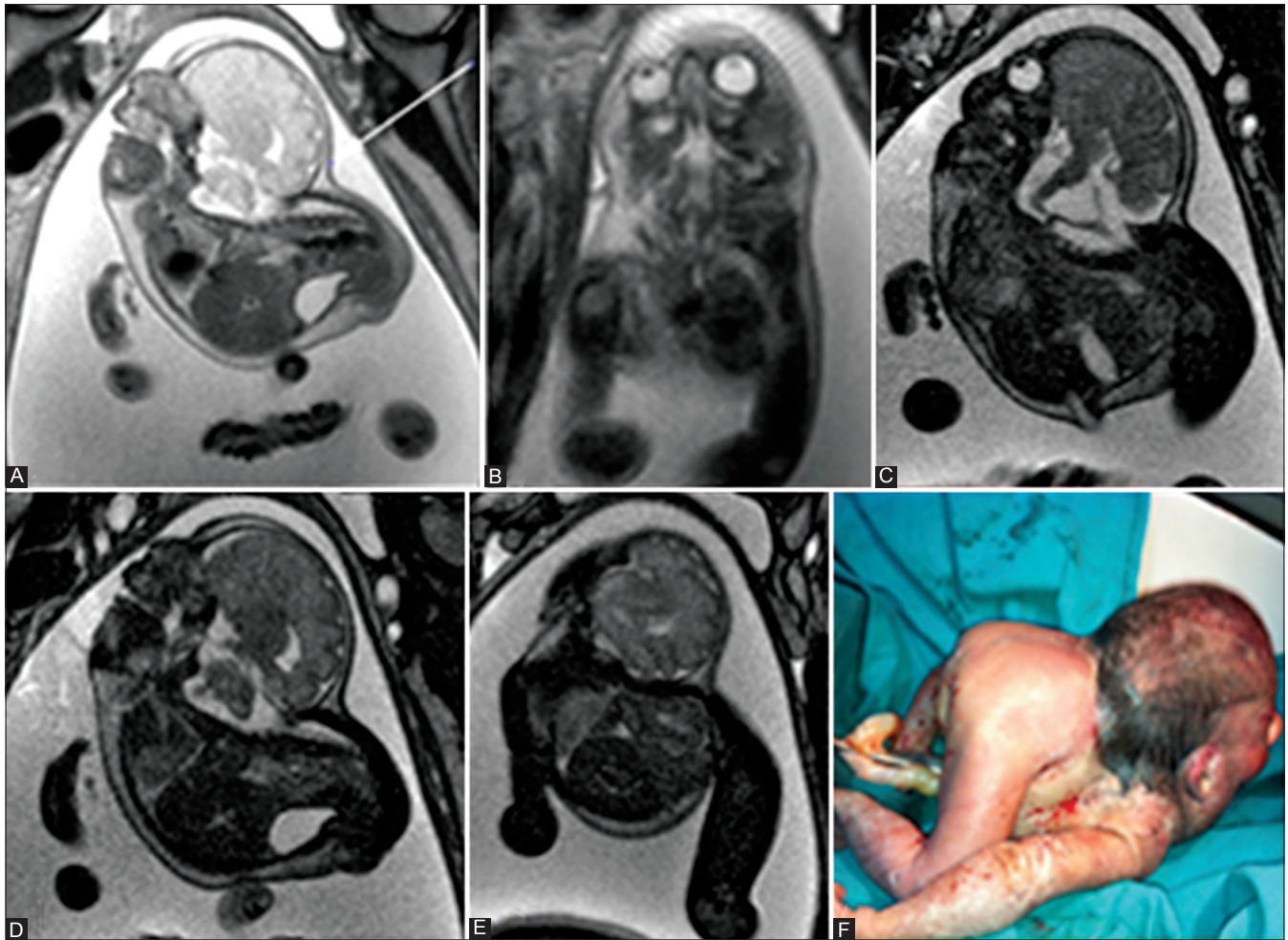


Figure 6 (A-F): Iniencephaly in a fetus at 29 weeks. T2W sagittal image, (A) BTFE s image coronal, (B) BTFE sagittal (C) and postnatal image (D) show fusion of head with the chest, occipital bone defect, total absence of cervico-thoracic vertebrae, and fixed fetal head retroflexion

helps in diagnosing PUVs with associated hydronephrosis or renal dysplasia.

Congenital megaureter

An infantile ureter measuring more than 7 mm, visualized as a hyperintense tubular structure posterior to the bladder on T2W sequences is termed as a megaureter.^[13] It can be further classified as obstructed primary megaureter, refluxing primary megaureter (vesicoureteric reflux), and non-refluxing obstructed primary megaureter.^[13]

Antenatally, this is seen as a dilated collecting system and ureter [Figure 9], as was seen in a 25-week pregnancy in our series. Reflux maybe excluded postnatally.

Multicystic dysplastic kidney

In multicystic dysplastic kidneys [Figure 10], multiple small non-communicating cysts are seen dispersed throughout the renal parenchyma. It usually affects one kidney with associated renal abnormalities like vesicoureteric reflux, pelviureteric junction obstruction, ureteral ectopia, and ureterocele in the contralateral

kidney.^[14] The non-communication of the cysts helps differentiating it from hydronephrosis.

Chest anomalies

Fetal lungs appear hyperintense on T2W and BTFE images. Common fetal thoracic anomalies are congenital diaphragmatic hernia (CDH), congenital pulmonary airway malformations (CPAM), and bronchopulmonary sequestration (BPS).^[15]

Lung volume is calculated on USG by lung to head ratio (LHR); if it is >1.6, survival is >83%. In MRI, total fetal lung volumes (TFLV) can be calculated. Cannie *et al.*^[16] conducted a study in 200 fetuses without abnormalities at University Hospital Gasthuisberg (Belgium). Total lung volume correlated best with fetal body volume (FBV) than with all other biometric variables. The estimated lung volume ELV is calculated by the equation: $ELV = [(2.0 \times 10^{-9}) \times FBV^3] - [(1.19 \times 10^{-5}) \times FBV^2] + (0.0508 \times FBV) - 1.79$. All fetuses with values < 14.3% have a 100% mortality rate and those with values >32.8 have a 100% survival rate.^[16] Thus, MRI scores over USG in calculating the lung

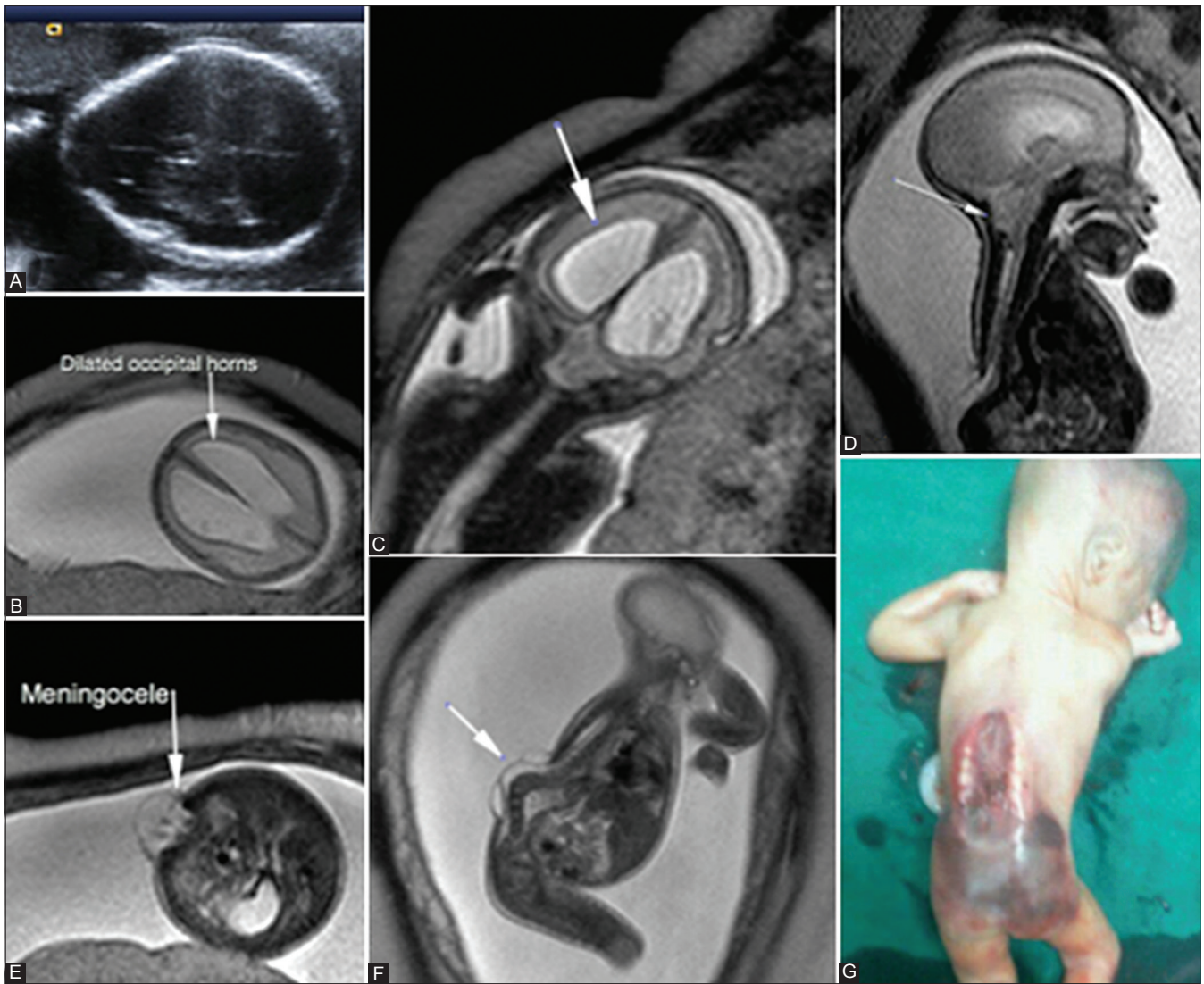


Figure 7 (A-G): (A) Arnold Chiari III malformation at 18 weeks gestation. Axial USG image shows lemon shaped skull, T2WI axial (B) reveal dilated ventricles, coronal T2WI, (C) and sagittal BTFE (D) images show colpocephaly and hydrocephalus. MRI revealed tonsillar herniation which could not be detected on ultrasound. Axial BTFE, (E) sagittal T2WI, (F) and postnatal (G) images show protrusion of CSF and meninges through a dorsal spinal defect into the subcutaneous plane in the lumbosacral region suggestive of meningocele

volume more accurately and, therefore, predicting the fetal outcome.^[16]

Congenital diaphragmatic hernia

In CDH, the diaphragm is incompletely formed resulting in a defect through which the contents of the abdomen can enter the thoracic cavity [Figure 11]. Left-sided diaphragmatic hernias are more common than right-sided ones, with omental fat, stomach, and small bowel loops being the commonest structures to herniate. In addition to more accurate evaluation of residual lung volume, MRI assesses the contents of the hernia more accurately than USG, hence determining the outcome.

Congenital pulmonary airway malformations

They are abnormal pulmonary solid/cystic masses vascularized by the pulmonary artery and drained via

pulmonary veins. Stocker *et al.*^[17] classified them as: Type I (one or more cysts >2 cm), type II (multiple cysts 2-0.5 cm), and type III (large microcystic lesion <0.5 cm). CPAMs appear hyperintense on T2WI than the normal lung parenchyma.

Bronchogenic cysts

These are congenital malformations of the bronchial tree (type of bronchopulmonary foregut malformation) appearing as large solitary cystic lesions. Most bronchogenic cysts appear as single lesions typically located in the mediastinum [Figure 12], in the carinal region, but can also be found in the lung parenchyma or extend below the diaphragm as dumbbell-shaped cysts.^[18]

Cystic hygromas

They are known as vasculolymphatic origin anomalies.^[19] They can arise anywhere along the lymphatic system; however,

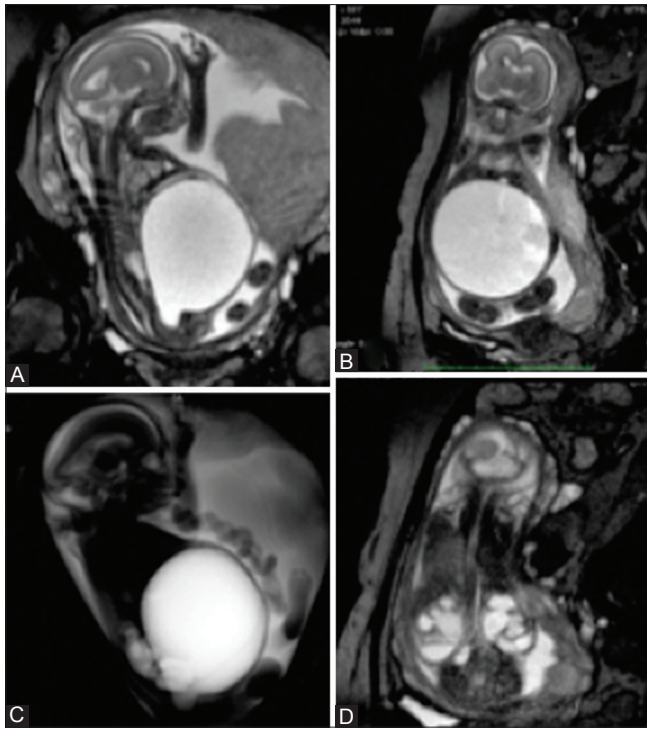


Figure 8 (A-D): Bilateral hydronephrosis due to posterior urethral valves at 23 weeks gestation. Sagittal T2W, (A) coronal T2W, (B) single shot T2W, (C) and T2W coronal (D) images show grossly distended urinary bladder causing elevation of the diaphragm, occupying the whole abdomen. Dilated posterior urethra and bilateral hydronephrosis is seen

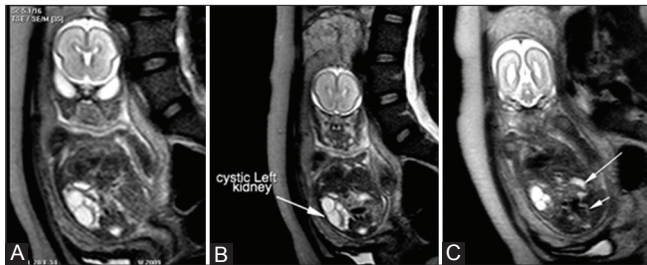


Figure 10 (A-C): Left multicystic dysplastic kidney with right hydronephrosis and hydronephrosis in a fetus at 22 weeks. USG suggestive of bulky left multicystic dysplastic kidney, non-visualized right kidney, and urinary bladder with severe oligohydramnios. T2W coronal, (A) BTFE coronal (B) and BTFE coronal images, (C) detected the presence of right kidney with hydronephrosis, hydronephrosis, and normal urinary bladder, and confirmed dysplastic left kidney

in most cases, they are located in the head and neck region. Cystic hygromas are multilobulated, thin-walled, lymph-containing sacs [Figure 13].

Other anomalies

Amniotic band syndrome

These are a group of congenital anomalies affecting the limbs and internal organs due to early rupture of amnion leading to fibrous bands with entrapment and herniation of the fetal parts^[20][Figure 14]. Multiple

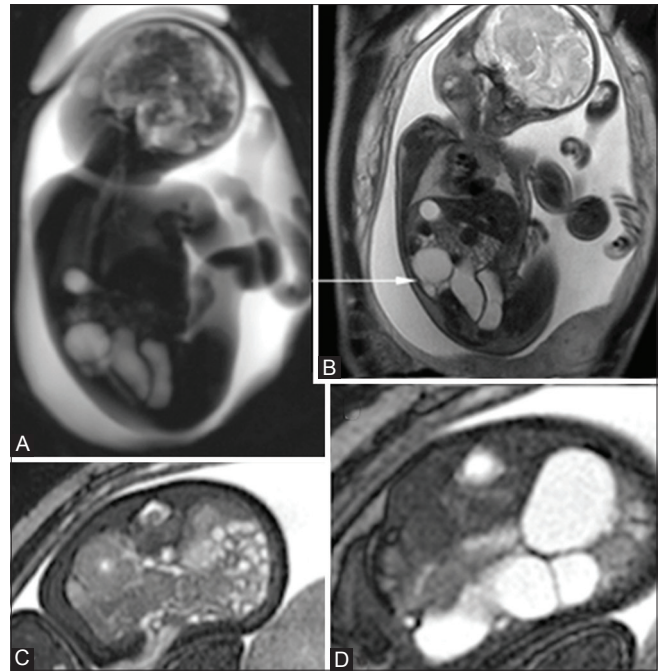


Figure 9 (A-D): Left hydronephrosis and megaureter in a fetus at 25 weeks. Single-shot coronal, (A) T2WI coronal, (B) BTFE axial (C and D) images show tortuous left megaureter measuring 18.5 mm. Left UV junction is narrowed with hydronephrotic left kidney and enlarged right kidney. Urinary bladder is normal

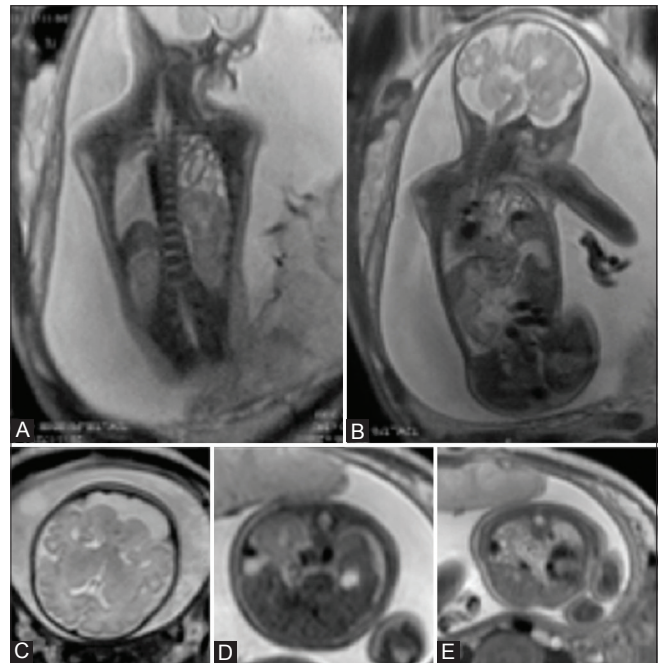


Figure 11 (A-E): Congenital diaphragmatic hernia and Dandy Walker variant in a fetus at 33 weeks. T2WI coronal (A and B) images show a diaphragmatic defect with herniation of bowel loops into the left hemithorax. T2W axial image (C) shows a giant cisterna magna. Right pleural effusion is also noted. T2WI axial images (D and E) show diaphragmatic hernias

amniotic bands maybe associated with colpocephaly due to CC dysgenesis.

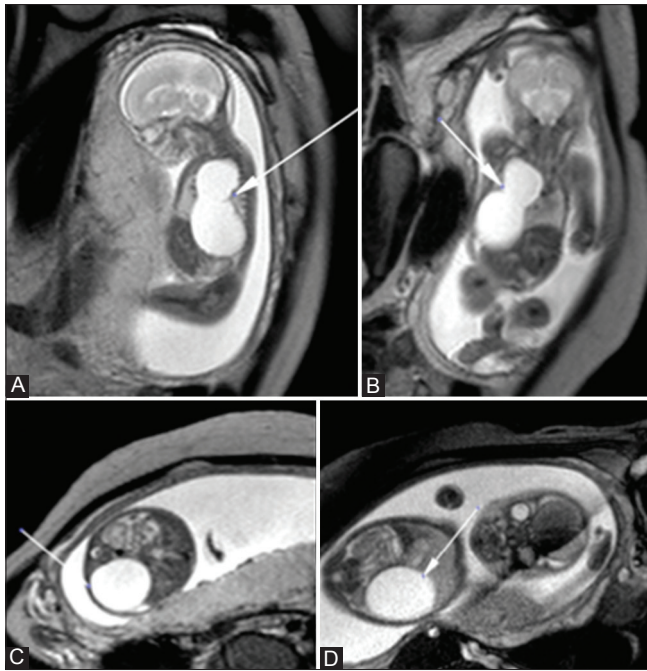


Figure 12 (A-D): Intrathoracic cyst/Bronchogenic cyst/CPAM type I or IV in a fetus at 22 weeks. T2WI sagittal, (A) coronal, (B and C) and axial (D) images showing 5.7 × 3 cm cystic mass occupying right hemithorax, causing diaphragmatic inversion and lung compression with thoracic scoliosis. In addition to it, MRI revealed ascites and bilateral pleural effusion

Congenital vascular malformations

These are a group of congenital dysplasias affecting the arterial, capillary, or venous system, presenting at birth. Sturge Weber, Klippel–Trenaunay, Maffucci, and Proteus syndromes are a few of these complex malformations.

Klippel–Trenaunay syndrome [Figure 15] comprises bony or soft tissue hypertrophy (localized gigantism), venous malformations, and port wine hemangiomas.^[21]

Twin pregnancies

Miscellaneous conditions were seen in twin pregnancies including conjoint twins, genitourinary anomalies (renal agenesis) involving one twin [Figure 16], dilated PUVs [Figure 17], and twin reversed arterial perfusion sequence (TRAP) syndrome.

TRAP sequence

It is seen in multifetal monochorionic pregnancies. It consists of abnormalities resulting from entrapment of various fetal parts from a disrupted amnion. The condition results in one normal (pump) twin and abnormal (acardiac) co-twin^[22] [Figure 18]. The acardiac twin is further classified as acardiusanceps (when the head is poorly formed), acardiusacephalus (if the head

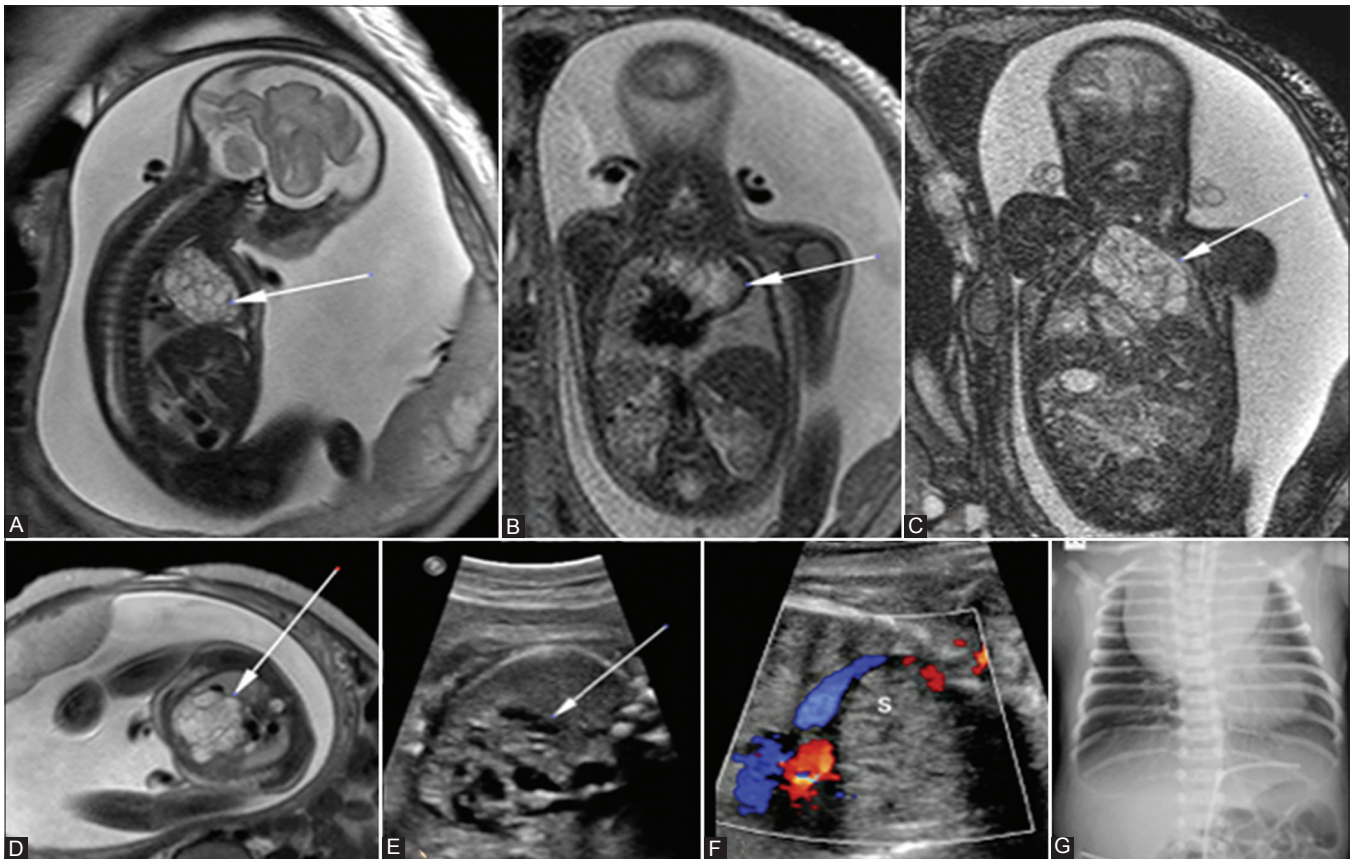


Figure 13 (A-G): Cystic hygroma in a fetus at 31 weeks. T2WI sagittal, (A) and BTFE coronal, (B and C) axial T2WI (D) images showing large multiloculated cystic midline mediastinal mass compressing and displacing the great vessels. Prenatal USG (E and F) revealed multiple cystic lesions in the anterior mediastinum. Postnatal X-ray (G) showed anterior mediastinal widening

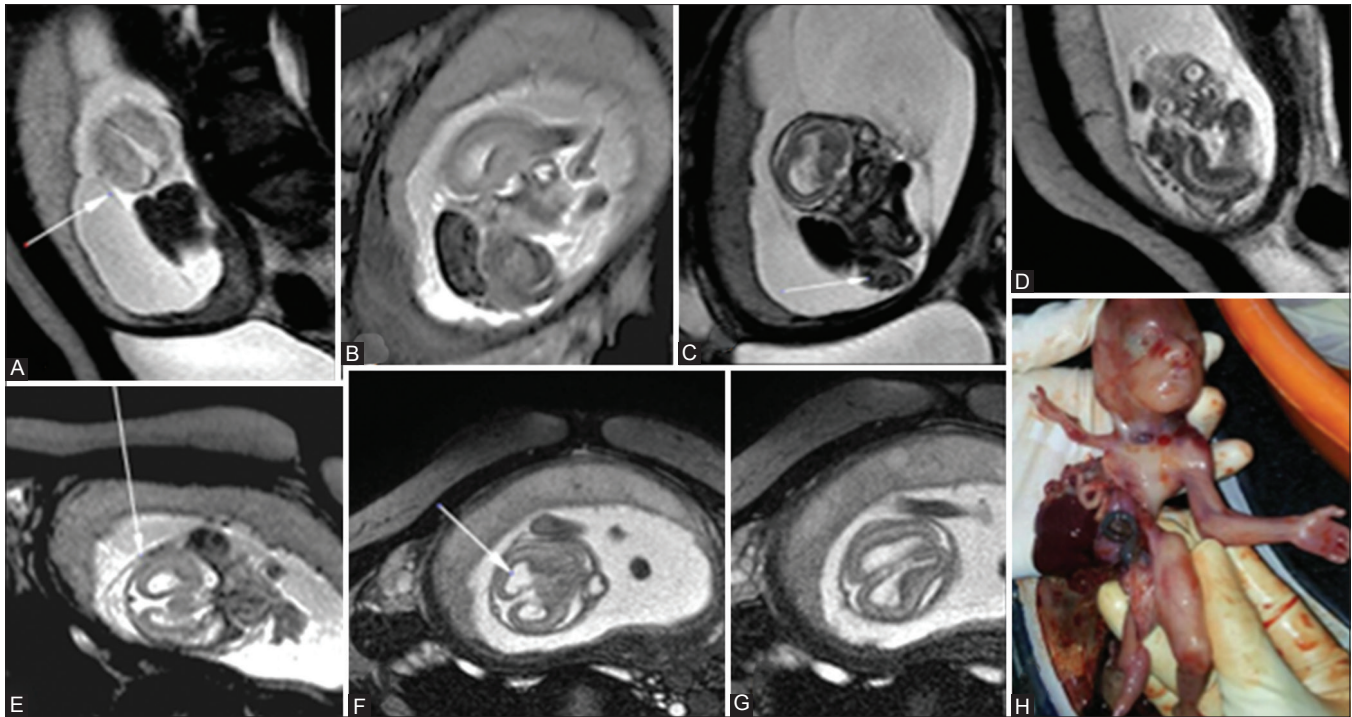


Figure 14 (A-G):Amniotic band syndrome in a fetus at 18 weeks. Maternal T2WI sagittal, axial and oblique coronal images(A-D and E-G) show multiple amniotic bands with fetus trapped in persistent hyperflexion. Herniation of abdominal contents limited by amniotic membrane. Additional MRI findings:Dilated lateral ventricles (colpocephaly), absent corpus callosum. (H) Autopsy specimen

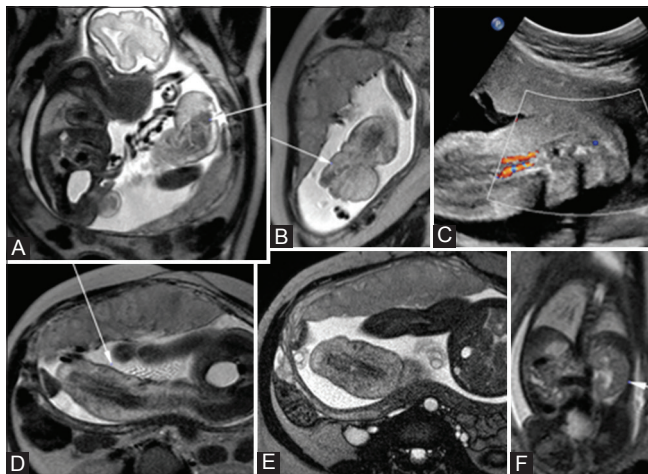


Figure 15 (A-F): Venous/lymphatic malformation and Klippel-Trenaunay-Weber syndrome at 28 weeks gestation. T2W coronal, (A and B) Coronal USG, (C) T2W sagittal (D) images show hyperintense subcutaneous soft tissues in right lower limb with extension into the gluteal region and T2W coronal (F) image shows bulky kidneys

is absent), acardiusacormus (presence of head only), and acardiusamorphous (unrecognizable amorphous mass).^[23]

Placental anomalies

Placenta previa, accreta, increta, and hydatiform molar pregnancy with live fetus [Figure 19] were few of the placental indications for performing fetal MRI.

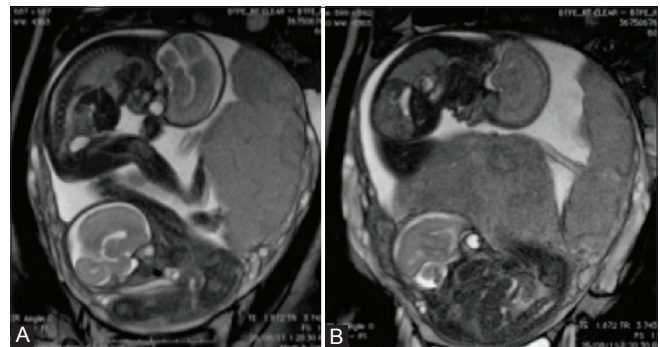


Figure 16 (A and B): Diamnioticdichorionic twin pregnancy with renal agenesis in presenting twin. T2W sagittal (A and B) images show presence of kidneys with distended bladder in the more cranial twin B. Distended bladder/both kidneys could not be demonstrated in the “presenting” more caudally placed fetus, twin A

Conclusion

The main role of MRI was to confirm/exclude lesions suspected on USG, as well as to define their extent and demonstrate associated abnormalities.

Fetal MRI scored over USG due to its higher spatial resolution, larger field of view, and ability to visualize fetal anatomy well, despite scanty liquor. Maternal factors such as echogenic abdominal wall and obesity are also not deterrents.

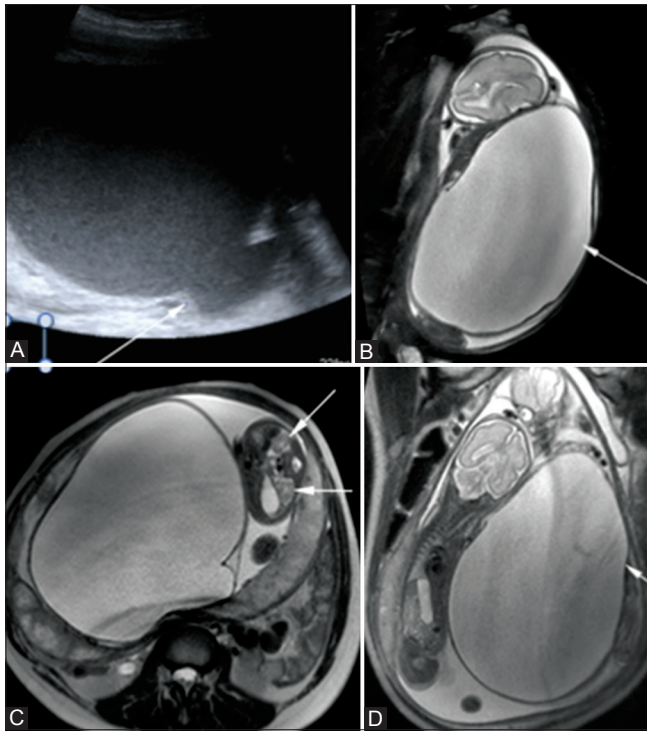


Figure 17 (A-D): Dilated PU valves in 26 weeks twin pregnancy. USG coronal (A) and T2WI (B-D) images show grossly distended urinary bladder of twin B. Normal twin A

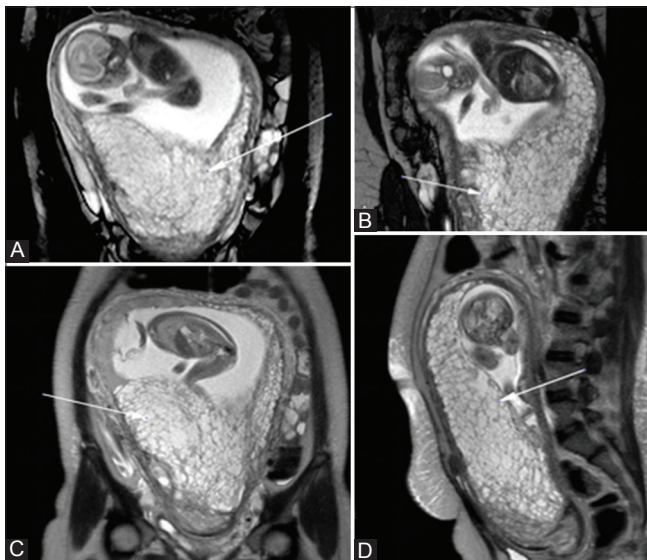


Figure 19 (A-D): Hydatiform molar pregnancy with a live fetus of 21 weeks. T2WI coronal (A) image shows normal fetus with multiple well-defined cystic areas seen caudal to the placenta covering the internal os (B and C) and T2WI axial to the fetus (D) shows normal stomach bubble and lungs with partial molar pregnancy

Fetal MRI is increasingly used in clinical practice, partly because of the increasing interest in fetal surgery and fetal medicine.^[24] It allows simultaneous imaging of different organ systems with reproducibility of images, producing images akin to postnatal scans, thus facilitating surgical

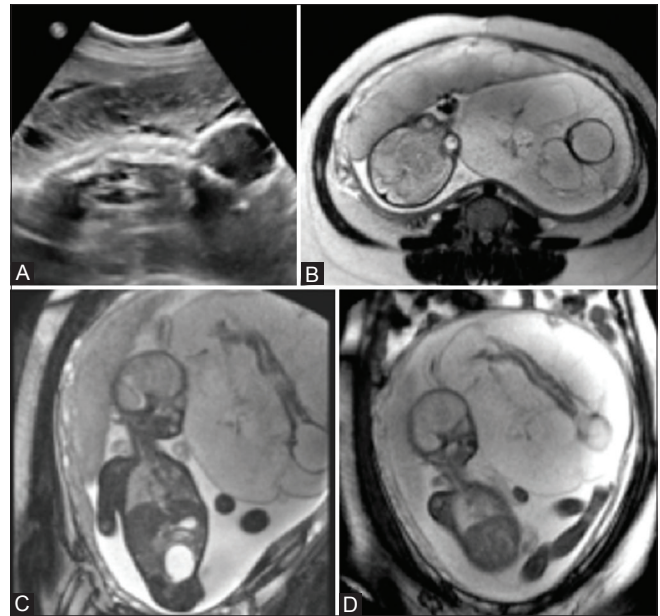


Figure 18 (A-D): Twin reversed arterial perfusion (TRAP) sequence. USG coronal image (A) shows lobulated mass and intracranial cystic lesion with deformed spine. T2WI coronal images, (B and C) and sagittal (D) images reveal acardius anceps (head is poorly formed) type of acardia twin and normal twin A

planning and intervention. It helps predict postnatal management and in genetic counseling.

Sequences such as DWI, Apparent Diffusion Coefficient, MRI spectroscopy, functional imaging, and volumetric data acquisition are still under research and show future promise.

Declaration of patient consent

The authors certify that they have obtained all appropriate patient consent forms. In the form the patient(s) has/have given his/her/their consent for his/her/their images and other clinical information to be reported in the journal. The patients understand that their names and initials will not be published and due efforts will be made to conceal their identity, but anonymity cannot be guaranteed.

References

1. Smith FW, Adam AH, Phillips WD. NMR imaging in pregnancy. *Lancet* 1983;1:61-2.
2. Levine D, Barnes PD, Sher S, Semelka RC, Li W, McArdle CR, et al. Fetal fast MR imaging: Reproducibility, technical quality, and conspicuity of anatomy. *Radiology* 1998;206:549-54.
3. Canto-Moreira N. MRI Studies of the Fetal Brain and Cranium. Uppsala; 2012. p. 53.
4. Shellock FG, Kanal E. Policies, guidelines, and recommendations for MR imaging safety and patient management. SMRIsafety committee. *J MagnReson Imaging* 1991;1:97-101.
5. Prayer D, Kasprian G, Krampfl E, Ulm B, Witzani L, Prayer L, et al. MRI of normal fetal brain development. *Eur J Radiol*

- 2006;57:199-216.
6. Kazi AZ, Joshi PC, Kelkar AB, Mahajan MS, Ghawate AS. MRI evaluation of pathologies affecting the corpus callosum: A pictorial essay. *Indian J Radiol Imaging* 2013;23:321-32.
 7. Sawhney S, Machado L, Jain R. Prenatal MRI image of a fetus with semilobar holoprosencephaly. *Sultan Qaboos Univ Med J* 2008;8:93-4.
 8. Pungavkar SA, Sainani NI, Karnik AS, Mohanty PH, Lawande MA, Patkar DP, *et al.* Antenatal diagnosis of iniencephaly: Sonographic and MR correlation: A case report. *Korean J Radiol* 2007;8:351-5.
 9. Sahid S, Sepulveda W, Dezerega V, Gutierrez J, Rodriguez L, Corral E. Iniencephaly: Prenatal diagnosis and management. *PrenatDiagn* 2000;20:202-5.
 10. Milhorat TH, Chou MW, Trinidad EM, Kula RW, Mandell M, Wolpert C, *et al.* Chiari I malformation redefined: Clinical and radiographic findings for 364 symptomatic patients. *Neurosurgery* 1999;44:1005-17.
 11. Kennedy WA. Assessment and management of fetal hydronephrosis. *Urology* 2002;10:214-9.
 12. Young HH, Frontz WA, Baldwin JC. Congenital obstruction of the posterior urethra. *J Urol* 1919;3:289-365.
 13. Berrocal T, López-Pereira P, Arjonilla A, Gutiérrez J. Anomalies of the distal ureter, bladder, and urethra in children: Embryologic, radiologic, and pathologic features. *Radiographics* 2002;22:1139-64.
 14. Aslam M, Watson AR; Trent and Anglia MCDK Study Group. Unilateral multicystic dysplastic kidney: Long term outcomes. *Arch Dis Child* 2006;91:820-3.
 15. Lee SY, Chari RS, Bhargava R. Fetal MRI in the evaluation of chest anomalies: A pictorial essay. *UAHSJ* 2006;3:27-30.
 16. Cannie MM, Jani JC, Van Kerkhove F, Meerschaert J, De Keyzer F, Lewi L, *et al.* Fetal body volume at MR imaging to quantify total fetal lung volume: Normal ranges. *Radiology* 2008;247:197-203.
 17. Stocker JT, Madewell JE, Drake RM. Congenital cystic adenomatoid malformation of the lung. Classification and morphologic spectrum. *Hum Pathol* 1977;8:155-71.
 18. Yoon YC, Lee KS, Kim TS, Kim J, Shim YM, Han J. Intrapulmonary bronchogenic cyst: CT and pathologic findings in five adult patients. *AJR Am J Roentgenol* 2002;179:167-70.
 19. Makariou E, Pikis A, Harley EH. Cystic hygroma of the neck: Association with a growing venous aneurysm. *AJNR Am J Neuroradiol* 2003;24:2102-4.
 20. Lockwood C, Ghidini A, Romero R. Amniotic band syndrome in monozygotic twins: Prenatal diagnosis and pathogenesis. *ObstetGynecol* 1988;71:1012-6.
 21. Phillips GN, Gordon DH, Martin EC, Haller JO, Casarella W. The Klippel-Trenaunay syndrome: Clinical and radiological aspects. *Radiology* 1978;128:429-34.
 22. Guimaraes CV, Kline-Fath BM, Linam LE, Garcia MA, Rubio EI, Lim FY. MRI findings in multifetal pregnancies complicated by twin reversed arterial perfusion sequence (TRAP). *Pediatr Radiol* 2011;41:694-701.
 23. Sebire NJ, Wong AE, Sepulveda W. Minimally invasive management of twin reversed arterial perfusion sequence (TRAP). *Fetal Matern Med Rev* 2006;17:1-22.
 24. Glenn OA, Coakley FV. MRI of the fetal central nervous system and body. *Clin Perinatol* 2009;36:273-300.

Cite this article as: Rathee S, Joshi P, Kelkar A, Seth N. Fetal MRI: A pictorial essay. *Indian J Radiol Imaging* 2016;26:52-62.

Source of Support: Nil, **Conflict of Interest:** None declared.